Vision-Based Lane Crossing Point Tracking for Motorcycles

Pierre-Marie Damon, Majda Fouka, Hicham Hadj-Abdelkader, Hichem Arioui

Vision-Based Lane Crossing Point Tracking for Motorcycles

Pierre-Marie Damon[1], Majda Fouka[1], Hicham Hadj-Abdelkader[1] and Hichem Arioui[1]

Abstract— **In this paper, we investigate a vision-based approach for online lane change prediction and detection dedicated Powered Two-Wheeled Vehicles. The approach is composed of two steps. First, the road geometry (clothoid model) and the motorcycle position with respect to the road markers are deduced based an inverse perspective mapping algorithm. The relative position is represented by the vehicle lateral displacement and heading estimated by means of an Inertial Measurement Unit and a monocular camera. The second step consists of predicting the Lane Crossing Point which allows to predict the distance and time before the motorcycle crosses the lane. The algorithm is achieved without the use of any steering sensor.**

To assess the effectiveness of the proposed approach, the estimation and the prediction schemes are validated on the BikeSim framework. To this end, two scenarios are discussed : 1- straight road with non-zero relative heading, and 2- curved road and circular vehicle trajectory.

I. Introduction

The study of the road accidents shows that the human factors (57%) appear far before the meteorological or technical issues [1]. The most frequent human causes: alcohol and speed are responsible respectively of 31% and 25% of fatal accidents. Distraction is also an important human factor in a road accident that can be highlighted by, for example, lane crossing or abnormal steering behavior. Hence, the prediction of the steering rider behavior is a crucial issue for Advanced River Assistance Systems (ARAS) to warn dangerous drive situations.

This work focuses on lane crossing prediction for powerred two-wheeled vehicles (P2WV). To the best of the author's knowledge, the problem has never been addressed for P2WV. The aim is to predict, whether a simple perception system, the spacial and temporal lane change information. Such information can be predicted uising the Time to Lane Crossing (TLC) and the Distance to Lane Crossing (DLC) which are key components to be estimated in order to predict critical situations.

Several safety systems for lane departure are already integrated in modern cars. Departure Lane Assist (DLA) systems make the vehicles more autonomous, allowing to inspect the surrounding vehicles position and to detect the driver hypo-vigilance. Lane detection can be done through different technologies [2]: Lane Departure Warning (LDW) system [3], Lane Keeping Assistance System (LKAS), etc. All those systems have been discussed, as well as their interoperability issue in [4], [5], [6], [7], [8].

[1] Authors are with University of Evry Val d'Essonne - Paris Saclay, IBISC Laboratory, Evry, France pierremarie.damon@univ-evry.fr

In some ways, the P2WV size can be seen as a weakness. They tend to frequently change travel direction and speed, regardless number of lanes or their width. Consequently, the lane crossing may create hazardous situations. To reduce safety risks, riders should try as much as possible to avoid the middle and the overtaking lanes since that would expose them to left side and right-side hazards posed by adjacent vehicles [9].

Currently, relevant works are planned to study the design of Lane Departure Warning for motorcycles from the control point of view [10]. In [11], the lane-keeping controller for motorcycles was evaluated through computer simulation with a rider-control model, in which the lane-following performance was improved by using a virtual-point regulator. In [12], the authors developed a Lane Change Decision aid system (LCDAS), which detects backward vehicles and motorcycles under weather and environmental. At the end, they used a change using single camera, in order to inform the driver of dangerous situations during lane change maneuvers. Futhermore, an optimal control theory to the lane keeping controller for motorcycles was presented in [13].

Nevertheless, there is a lack of literature review related to the problem of Lane Crossing Point (LCP) detection for motorcycles. Therefore, DLA systems for motorcycles need more thorough investigations to be embedded in modern two-wheelers.

The remaining of this paper is organized as follows. Section II motivates the paper's topics. Section III reviews our previous work on Inverse Persepctive Mapping (IPM) techniques for motorcycles. Section IV discusses the distance to lane crossing estimation. Whereas, sections V and VI present the results, conclude the paper and outline the future works.

II. Problem Statement

The detection and tracking of the LCP for motorcycles involve several technical problems that must be overcome. The Whereas prediction is realized in most cases through monocular cameras by reconstructing the road profile as well as the current position of the vehicle. This is also done under some assumptions such as flat roads and perfectly parallel markings.

In the case of motorcycle riding, both previous assumptions are violated because of a bike dynamics. Indeed, the P2WV can reach significant roll angles (the world record is about $68°$) and undergo load transfers during braking or acceleration phases (pitch angle significant). Following this, the images recorded by the front camera undergo noteworthy deformations and do not allow a direct use without

a projection in a more advantageous plan (bird-eye-view for example). The next section recalls our previous work on a vision based approach for accurate vehicle position reconstruction.

This allows to recover crucial information such that the DLC or the TLC which are both proportional regarding the vehicle speed. The second step presents the algorithm able of tracking the LCP.

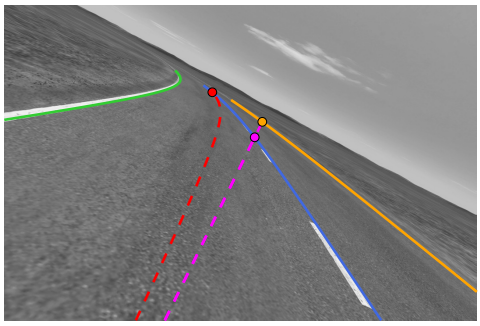

Fig. 1: Captured camera image with reprojected road lanes, predicted trajectories and LCP

III. Vision-based information

The contribution of this paper is based on the results initially introduced in [14]. The reader could refer to the following videos https://www.youtube.com/playlist?list=PLRTI62SuvNymK2Dx-YKha-1a4Sp54IVs8 for visual illustrations. In [14], the authors used the IPM technique combined with a road lanes filter allowing to generate a bird-eye-view of the road markers (as presented in figure 3). Then, a clothoid model of the road is used to extract pertinent information such that the P2WV relative lateral displacement and heading angle to the road markers. They are respectively denoted ΔY_i and $\Delta\psi_i$, where $i \in \{l, c, r\}$ indicates left, center and right markers. It allows to recover crucial information regarding the P2WV location on the road.

Furthermore, the clothoid model allows to predict the road curvature and its rate respectively named C_0 and C_1. Both parametres allow to faithfully reconstruct the road trajectory in the selected Region Of Interest (ROI). Note that, even if the ROI limit ahead of the P2WV is chosen about 30 meters (see [14]), each road marker trajectory can be extended since we know its third degree polynomial approximation.

Let us remind that each road lane is approximated in the cartesian coordinate system with the following expression for $i \in \{l, c, r\}$:

$$y_i(x) \approx \Delta Y_i + \tan(\Delta\psi_i)x + \frac{1}{2}C_{0_i}x^2 + \frac{1}{6}C_{1_i}x^3 \qquad (1)$$

Whereas, in the simulations discussed in [14], the right road marker is defined as a static reference, we proposed to introduce a dynamic reference. Indeed, the accuracy of the lane i trajectory reconstruction mainly depends on two factors: the proximity with this lane and its attribute (dashed or solid). Our strategy is to choose the reference among the right or left solid lanes regarding the estimated P2WV position on the road (given by ΔY and $\Delta\psi$). Note that, choose the center marker is depreciated because it is often discontinuous leading to less accurate approximation. Then, if the P2WV is traveling in the right (respectively left) lane, the right (respectively left) road marker is set as the reference. Finally, since the road markers are assumed parallel and separated from each other by a distance L, the two others lanes trajectories are reconstructed from the reference road marker equation (1). At this point, we know an estimation of the three lanes trajectories in the vehicle frame F_v whose the origin is the projection of the camera center on the ground.

IV. Lane crossing point tracking

Now, considering that the road lane trajectories are available, the LCP tracking problem consists of finding the intersection point coordinates between the predicted road lane and vehicle trajectories. For the latter, we addressed two cases. For both the vehicle speed is assumed constant and positive. The first case considers a straight predicted vehicle trajectory which corresponds to a zero steering angle ($\delta = 0$). Whereas for the second, δ is assumed constant and non zero. Under these last assumptions, the predicted vehicle trajectory is a circular path with a constant radius. For what follows, we denoted DLC_0 and DLC_δ the predicted distances to the LCP respectively for straight and circular vehicle trajectories. Note that, the DLC is computed with respect to the vertical projection of the camera center on the ground which is the origin of the frame F_v.

Note that, for the case where $\delta \neq 0$ (the rider is steering), we systematically compute two DLC which are DLC_0 and DLC_δ. The first considering a straight predicted trajectory and the second based on a circular path prediction (see figure 3). This allows to get a surface containing all the LCP between the actual circular path and the straight one. In other words, it provides indications about the LCP location in case of the rider reduces the steering (increase of the trajectory radius).

Moreover, for both scenarios ($\delta = 0$ and $\delta \neq 0$), we solved the DLC algorithm for each detected road lane. Hence, the final LCP is the nearest point among the solutions as illustrated in figure 1 and 3.

A. Straight predicted vehicle trajectory ($\delta = 0$)

For straight predicted path, the computation of the DLC can be easily achieved by solving the equations for $i \in \{l, c, r\}$:

$$\Delta Y_i + \tan(\Delta\psi_i)x + \frac{1}{2}C_{0_i}x^2 + \frac{1}{6}C_{1_i}x^3 = 0 \qquad (2)$$

Let us remind (2) is expressed in the vehicle frame F_v where X_v corresponds to the vehicle longitudinal axis (refer to 3). Hence, if $x_{DLC_{0_i}}$ is a solution of equation (2) then, the DLC with regards to the lane i is trivial. It can be directly

deduced such that: $DLC_{0_i} = x_{DLC_{0_i}}$. Let us remind, the final DLC is computed such that $DLC_0 = \min(DLC_{0_k})$ with k corresponding to the set of all the lane intersection points. In figure 3, the magenta line clearly illustrates the situation with $k = \{\text{center}, \text{right}\}$.

B. Circular predicted vehicle trajectory ($\delta \neq 0$)

In this case, we need to reconstruct the forward predicted vehicle trajectory based on its current dynamic states. To do so, it requires to compute the vehicle slip angle denoted ψ_s. It can be expressed as a function of the the measured yaw angle (ψ) and the angle of the trajectory tangential vector (ψ_t) as illustrated in figure 2.

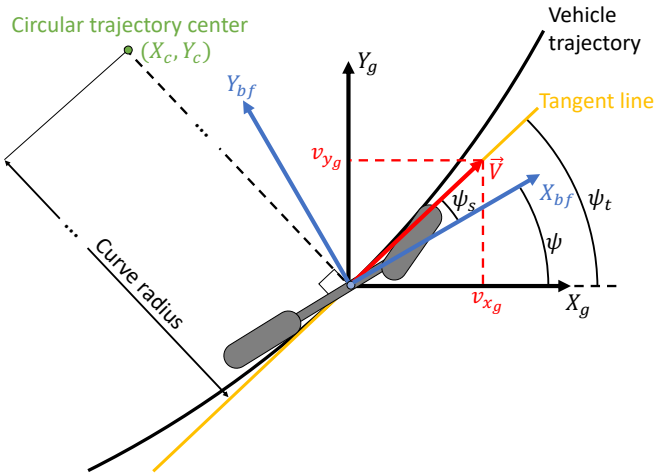

Fig. 2: Scheme of the vehicle circular path prediction

Now, let us consider that the yaw angle, measured by the IMU, is included in the interval $[-\pi, \pi]$. To avoid any singularity, we introduced the following relation:

$$\begin{aligned} \psi_s &= \Psi_t(\psi, \psi_t) - \Psi(\psi) \\ &= \psi_t + \pi \text{sign}\left(\Psi(\psi)\right) \Theta\left(\psi_t, \psi\right) - \Psi(\psi) \end{aligned} \tag{3}$$

with Θ and Ψ defined by the following functions:

$$\Psi(\psi) = \begin{cases} \psi - \text{sign}(\psi)\pi/2 & \text{if } |\psi| \geq \pi/2 \\ \psi & \text{if } |\psi| < \pi/2 \end{cases} \tag{4}$$

and

$$\Theta\left(\psi_t, \psi\right) = \begin{cases} 0 & \text{if } \left|\psi_t - \Psi(\psi)\right| \leq \pi/2 \\ 1 & \text{if } \left|\psi_t - \Psi(\psi)\right| > \pi/2 \end{cases} \tag{5}$$

At this step, the aim is to express ψ_t as a function of the IMU measurements such that the body-fixed accelerations ($a_{x_{bf}}$, $a_{y_{bf}}$, $a_{z_{bf}}$) and the orientation angles (ϕ, θ, ψ).

Let us define $A_j = [a_{x_j}, a_{y_j}, a_{z_j}]^T$ and $V_j = [v_{x_j}, v_{y_j}, v_{z_j}]^T$ as the acceleration and the speed vectors with $j = g$ for the global frame and $j = bf$ for the body-fixed one. Let us remind the following relations between the two frames:

$$\begin{cases} V_g &= \mathcal{R} V_{bf} \\ A_g &= \mathcal{R} A_{bf} \end{cases} \tag{6}$$

where $\mathcal{R} = \mathcal{R}_\psi \mathcal{R}_\theta \mathcal{R}_\Phi$ is the rotation matrix. The terms $\mathcal{R}_\psi$, $\mathcal{R}_\theta$ and $\mathcal{R}_\Phi$ denote the rotation matrices associated respectively to the yaw, pitch and roll Euler angles. Note that Φ is the rotation angle about the axis which has been previously pitched of θ. The real vehicle roll angle, denoted ϕ, can be computed using the algebraic expression:

$$\phi = \text{asin}\left(\cos(\theta)\sin(\Phi)\right) \tag{7}$$

Furthermore, the acceleration vector in the global frame can be obtain with the relation: $A_g = \dot{V}_g$. Combining the latter and (6) leads to:

$$A_g = \dot{\mathcal{R}} V_{bf} + \mathcal{R} \dot{V}_{bf} \tag{8}$$

Since we assumed the vehicle motion is uniform and circular ($\Phi = cst$, $\theta = cst$, $\dot{V}_{bf} = 0$), equation (8) can be reduced to:

$$A_g = \dot{\mathcal{R}} V_{bf} \tag{9}$$

where $\dot{\mathcal{R}} = \dot{\mathcal{R}}_\psi \mathcal{R}_\theta \mathcal{R}_\Phi$ is the time derivative of the rotation matrix.

Using equations (6) and (9), we obtain the following expression:

$$\begin{aligned} \mathcal{R} A_{bf} &= \dot{\mathcal{R}} V_{bf} \\ &= \dot{\mathcal{R}} \mathcal{R}^{-1} V_g \end{aligned} \tag{10}$$

Afterwards, we get one expression of the speed vector in the global frame:

$$V_g = \mathcal{M} A_{bf} \tag{11}$$

where $\mathcal{M} = \mathcal{R}\dot{\mathcal{R}}^{-1}\mathcal{R} = [m_{ij}]$ with $i, j \in \{1, 2, 3\}$

Let us remind that, by definition, the speed vector, expressed in the global frame, is tangent to the vehicle trajectory. Since ψ_t is the angle of the tangential direction to the P2WV trajectory, it comes:

$$\begin{aligned} \psi_t &= \text{atan}\left(\frac{v_{y_g}}{v_{x_g}}\right) \\ &= \text{atan}\left(\frac{m_{21}a_{x_{bf}} + m_{22}a_{y_{bf}} + m_{23}a_{z_{bf}}}{m_{11}a_{x_{bf}} + m_{12}a_{y_{bf}} + m_{13}a_{z_{bf}}}\right) \end{aligned} \tag{12}$$

with:

$$\begin{aligned} m_{11} &= \sin(\psi)\cos(\theta) \\ m_{12} &= \cos(\psi)\cos(\Phi) + \sin(\psi)\sin(\theta)\sin(\Phi) \\ m_{13} &= -\cos(\psi)\sin(\Phi) + \sin(\psi)\sin(\theta)\cos(\Phi) \\ m_{21} &= -\cos(\psi)\cos(\theta) \\ m_{22} &= \sin(\psi)\cos(\Phi) - \cos(\psi)\sin(\theta)\sin(\Phi) \\ m_{23} &= -\sin(\psi)\sin(\Phi) - \cos(\psi)\sin(\theta)\cos(\Phi) \end{aligned}$$

At this point, the vehicle slip angle denoted ψ_s can be computed using equations (3), (4), (5), (7) and (12).

Now, let us consider the IMU measurements, A_{bf} and $\dot{\psi}$, are given at a fixed sample rate denoted Δt. Then, under the previous assumptions, at an instant t, the vehicle trajectory, defined by $\hat{X}_{vh}$ and $\hat{Y}_{vh}$, can be predicted with the algorithm 1.

Algorithm 1 Motorcycle circular trajectory prediction

Inputs:
ψ_s, $\dot{\psi}$, A_{bf}, Δt
Outputs:
$\hat{X}_{vh}$, $\hat{Y}_{vh}$
Initialization:
$D_{\Delta t} \leftarrow \dfrac{\|A_{bf}\|}{\left|\dot{\psi}\right|}\Delta t$,
$\Delta\psi^1 \leftarrow -\psi_s$,
$\hat{X}^1_{vh} \leftarrow 0$,
$\hat{Y}^1_{vh} \leftarrow 0$
for i = 2 to $\dfrac{\pi}{2\left|\dot{\psi}(t)\right|\Delta t} + 1$ **do**
  $\Delta\psi^i \leftarrow \Delta\psi^{i-1} - \dot{\psi}(t)\Delta t$
  $\hat{X}^i_{vh} \leftarrow D_{\Delta t}\cos\left(\Delta\psi^i\right) + \hat{X}^{i-1}_{vh}$
  $\hat{Y}^i_{vh} \leftarrow D_{\Delta t}\sin\left(\Delta\psi^i\right) + \hat{Y}^{i-1}_{vh}$
end for

Note that, algorithm 1 predicts the discrete vehicle trajectory from its current position to the one with an angular horizon of $\pi/2$. The term $D_{\Delta t}$ denotes the constant traveled distance along the circular path during Δt. Since the vehicle motion is assumed circular, uniform and forward, it comes:

$$V_{bf} = \frac{\|A_{bf}\|}{\left|\dot{\psi}\right|} \tag{13}$$

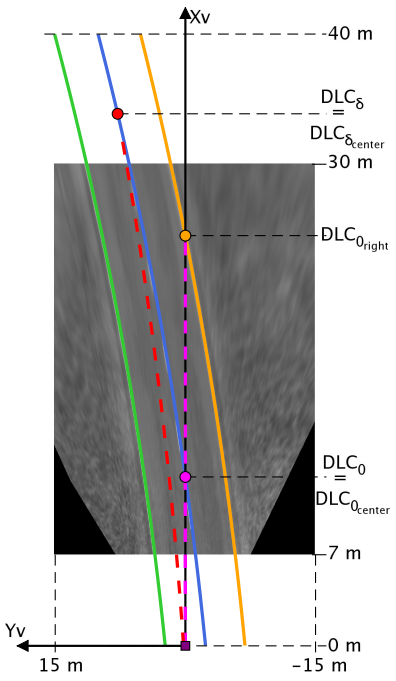

Fig. 3: Road bird-eye-view with predicted vehicle trajectories and tracked LCP

Finally, in this case of non zero steering, the DLC is the numerical solution when solving the intersection between the road lane equations (1) and the discrete predicted trajectory given by algorithm 1 (see the red dot in figure 3). As for straight path, when several LCP are detected then $DLC_\delta = \min(DLC_{\delta_k})$ with k a set of all LCP.

Notice that, since the longitudinal vehicle speed is available, the DLC can be trivially turned into a TLC using the expression:

$$TLC = \frac{DLC}{v_{x_{bf}}} \tag{14}$$

V. Simulation Results

This section discusses a validation of the proposed algorithm using the advanced motorcycle simulator BikeSim. Two scenarios are presented, the first one considers straight road and motorcycle trajectories with a constant relative heading deviation ($\Delta\psi \neq 0$). Whereas, the second scenario deals with circular road and vehicle trajectories ($\delta \neq 0$).

The hardware (camera and IMU) specifications and mountings are identical to the ones given in [14] except the camera resolution which is 1080×720. Let us remind the ROI of the bird-eye-view is limited about 30 meters ahead of the vehicle. According to the fact that the road trajectory is slowly varying, we extended the road lane reconstruction to 40 meters that we defined as the maximum horizon for LCP tracking.

In the following simulations, we considered a two-way road separated with a dashed road marker whereas the extreme lanes are continued.

A. Case 1 : Straight road with zero steering

In this scenario, we considered straight road markers and we simulated a constant heading deviation angle between the road lanes and the vehicle such that $\Delta\psi = 3°$. In addition, the P2WV is traveling at 100 km/h without any steering action.

Figure 4-a and 4-b illustrate the simulated trajectory of the motorcycle as well as the lateral deviation with adjacent lanes (central and left one). From 0 to 75 first meters, on X axis, the P2WV reaches the first Lane Crossing Point with the central line within 3 seconds. The vehicle travels under the same conditions (DLC & TLC) the second portion, but this time between the center lane and the left one.

Figure 4-c gives the estimated DLC for the case of a pure longitudinal movement respectively with the central and left lanes. A comparison with the theoretical DLC, expressed by the equations 2, is given. It shows well the approximation of the DLC by our approach, although the resolution is not very high with a rather important speed, figure 4-d. Here, the average error is about 50 centimeters and decreases drastically when the LCP is approaching.

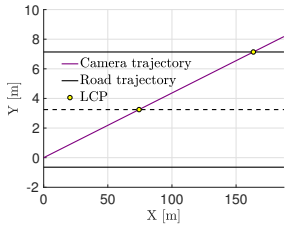

(a) P2WV trajectory

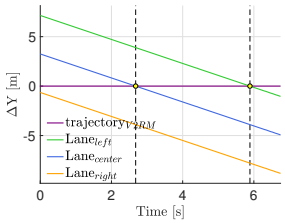

(b) Lateral displacement to the lane i in F_v

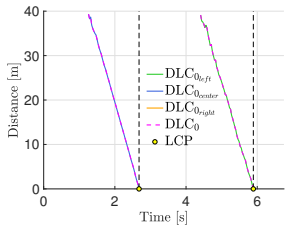

(c) Estimated DLC for zero steering

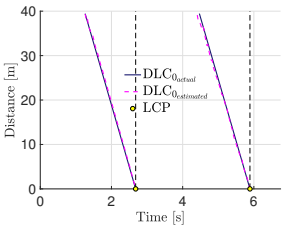

(d) Estimated vs actual DLC for zero steering

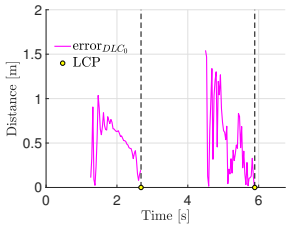

(e) DLC absolute error

Fig. 4: DLC for straight P2WV trajectory on straight road

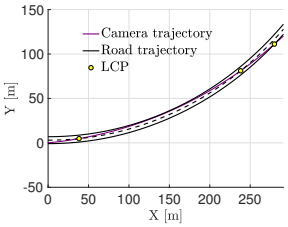

(a) P2WV trajectory

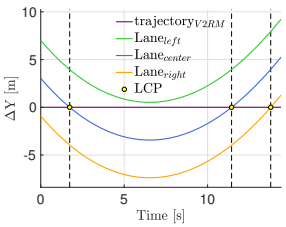

(b) Lateral displacement to the lane i in F_v

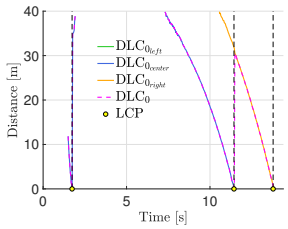

(c) Estimated DLC for zero steering

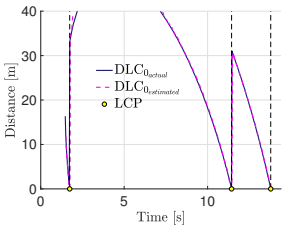

(d) Estimated vs actual DLC for zero steering

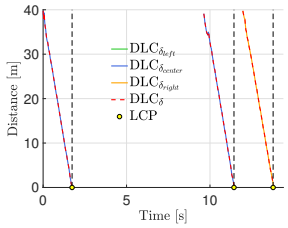

(e) Estimated DLC for constant steering

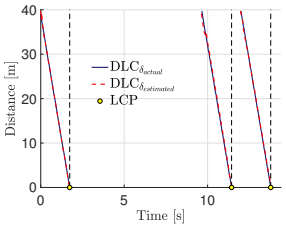

(f) Estimated vs actual DLC for constant steering

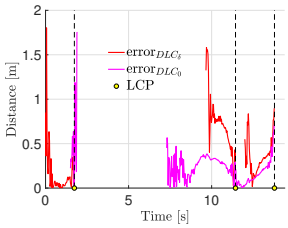

(g) DLC absolute error

Fig. 5: DLC for circular P2WV trajectory on curved road

B. Curved roads with constant steering

In the next scenario, we assume bend case with curve radius 400 meters and we simulated a constant steering angle, figure 5-a. The longitudinal speed is fixed at 80 km/h.

In the present scenario, three LCP are detected, figure 5-b. The last one occurs with the right lane and the remains LCP with the center lane.

Figure 5-c gives the reconstructed DLC for the case of a pure lateral motion respectively with the central and right lanes. Whereas, the estimated DLC is compared to the theoretical one under a zero steering. Figure 5-d highlights a very good estimation of the DLC. The estimation under constant steering is depicted in figures 5-e and 5-d to show, at the same time, the performance of the proposed algorithm. Also, the average error is similar to the previous scenario and remains around 50 centimeters and decreases when the LCP is approaching, figure 5-g. These results are illustrated by the video at the following link : https://youtu.be/K095a2SckWU.

VI. Conclusions and Future Works

This paper provided powerful video-based estimation algorithm for Lane Crossing Point tracking for powered two-wheeled vehicles. First we have recalled the Inverse Perspective Mapping technique, adapted to motorcycles, which allows the generation a bird-eye-view of the road markers. The advantage here is to extract pertinent information such that the P2WV lateral displacement and heading angle to the road marker. Second, the Lane Crossing Point tracking problem is detailed. It consists of finding the intersection point coordinates between the predicted road lane and vehicle trajectories whether straight or circular. Then, the proposed algorithm is simulated towards several scenarios to show its great capabilities of tracking road lanes and compute the distance before crossing the marker. Finally, the proposed algorithm is an original contribution which allows to accu-

rately compute, in real time, the DLC when lane change is occurring for motorcycles. This information is crucial for safety purposes like trajectory analysis.

In our future works, we plan to deal with the robustness (unfavorable camera light, undetected road markers, etc.) and to extend the algorithm to clothoid trajectories with various road curvature. We would like to take the proposed solution to the next step by integrating a risk function to create an alert system prototype. Finally, we would put all our effort into the experimental validation on our two-wheeled vehicle platform.

VII. Acknowledgement

This work is supported by National Agency of Research in France, under the framework VIROLO++ ANR-15-CE22-0008 : https://anr.fr/Projet-ANR-15-CE22-0008.

References

[1] A. P. Penumaka, G. Savino, N. Baldanzini, and M. Pierini, "In-depth investigations of ptw-car accidents caused by human errors," *Safety Science*, vol. 68, pp. 212 – 221, 2014. [Online]. Available: http://www.sciencedirect.com/science/article/pii/S0925753514000897

[2] D. Gonzalez Bautista, "Functional architecture for automated vehicles trajectory planning in complex environments," Theses, PSL Research University, Apr. 2017. [Online]. Available: https://pastel.archives-ouvertes.fr/tel-01568505

[3] C. Visvikis, T. Smith, M. Pitcher, and R. Smith, "Study on lane departure warning and lane change assistant systems," *Final Report, Transport research laboratory*, 2008, technical assistance and economic analysis in the filed of legislation pertinent to the issue of automotive safety PROJECT REPORT. [Online]. Available: http://www.sciencedirect.com/science/article/pii/S147466701638466X

[4] S. Mammar, S. Glaser, M. Netto, and J. . Blosseville, "Time-to-line crossing and vehicle dynamics for lane departure avoidance," in *Proceedings. The 7th International IEEE Conference on Intelligent Transportation Systems (IEEE Cat. No.04TH8749)*, Oct 2004, pp. 618–623.

[5] S. Mammar, S. Glaser, and M. Netto, "Time to line crossing for lane departure avoidance: a theoretical study and an experimental setting," *IEEE Transactions on Intelligent Transportation Systems*, vol. 7, no. 2, pp. 226–241, June 2006.

[6] W. Wang, D. Zhao, W. Han, and J. Xi, "A learning-based approach for lane departure warning systems with a personalized driver model," *IEEE Transactions on Vehicular Technology*, vol. 67, no. 10, pp. 9145–9157, Oct 2018.

[7] A. Benine-Neto, S. Scalzi, S. Mammar, M. Netto, and B. Lusetti, "Model reference-based vehicle lateral control for lane departure avoidance," *International Journal of Vehicle Autonomous Systems*, vol. 12, no. 3, pp. 284–306, 2014.

[8] S. Lefevre, Y. Gao, D. Vasquez, H. E. Tseng, R. Bajcsy, and F. Borrelli, "Lane keeping assistance with learning-based driver model and model predictive control," in *12th International Symposium on Advanced Vehicle Control*, 2013.

[9] N. F. P. A Hamzah, S Solah, "Motorcycles ?keep left? order: Is it viable?" in *Vehicle Safety and Biomechanics Research Centre, Malaysian Institute of Road Safety Research,Malaysia*, 2018.

[10] Y. Marumo and N. Katagiri, "Control effects of steer-by-wire system for motorcycles on lane-keeping performance," *Vehicle System Dynamics*, vol. 49, no. 8, pp. 1283–1298, 2011. [Online]. Available: https://doi.org/10.1080/00423114.2010.515030

[11] N. Katagiri, Y. Marumo, and H. Tsunashima, "Evaluating lane-keeping-assistance system for motorcycles by using rider-control model," in *SAE Technical Paper*. SAE International, 09 2008. [Online]. Available: https://doi.org/10.4271/2008-32-0056

[12] E. Y. Chung, H. C. Jung, E. Chang, and I. S. Lee, "Vision based for lane change decision aid system," in *2006 International Forum on Strategic Technology*, Oct 2006, pp. 10–13.

[13] N. Katagiri, Y. Marumo, and H. Tsunashima, "Controller design and evaluation of lane-keeping-assistance system for motorcycles," *Journal of mechanical systems for transportation and logistics*, vol. 2, no. 1, pp. 43–54, 2009.

[14] P. M. Damon, H. Hadj-Abdelkader, H. Arioui, and K. Youcef-Toumi, "Image-based lateral position, steering behavior estimation, and road curvature prediction for motorcycles," *Robotics and Automation Letters*, vol. 3, no. 3, pp. 2694–2701, July 2018.